

Hydrogen chemoresistive sensor for the analysis of gut health

*Original*

Hydrogen chemoresistive sensor for the analysis of gut health / Gullino, A.; Grassini, S.; Gugliandolo, G.; Moulaei, K.; Donato, N.; Parvis, M.; Lombardo, L.. - STAMPA. - (2021), pp. 1-6. ( 2021 IEEE International Symposium on Medical Measurements and Applications, MeMeA 2021 Lausanne, Switzerland (Virtual) 23-25 June 2021) [10.1109/MeMeA52024.2021.9478669].

*Availability:*

This version is available at: 11583/2971730 since: 2022-09-26T10:27:54Z

*Publisher:*

Institute of Electrical and Electronics Engineers Inc.

*Published*

DOI:10.1109/MeMeA52024.2021.9478669

*Terms of use:*

This article is made available under terms and conditions as specified in the corresponding bibliographic description in the repository

*Publisher copyright*

IEEE postprint/Author's Accepted Manuscript

©2021 IEEE. Personal use of this material is permitted. Permission from IEEE must be obtained for all other uses, in any current or future media, including reprinting/republishing this material for advertising or promotional purposes, creating new collecting works, for resale or lists, or reuse of any copyrighted component of this work in other works.

(Article begins on next page)

© 2021 IEEE. Personal use of this material is permitted. Permission from IEEE must be obtained for all other uses, in any current or future media, including reprinting/republishing this material for advertising or promotional purposes, creating new collective works, for resale or redistribution to servers or lists, or reuse of any copyrighted component of this work in other works.

## **Hydrogen chemoresistive sensor for the analysis of gut health**

Alessio Gullino

Dipartimento di Scienza Applicata e Tecnologia, Politecnico di Torino, Torino, ITALY

Sabrina Grassini

Dipartimento di Scienza Applicata e Tecnologia, Politecnico di Torino, Torino, ITALY

Giovanni Gugliandolo

Dipartimento MIFT, Università degli Studi di Messina, Messina, ITALY

Nicola Donato

Dipartimento di Ingegneria, Università degli Studi di Messina, Messina, ITALY

Kaveh Moulaei

Dipartimento di Ingegneria, Università degli Studi di Messina, Messina, ITALY

Marco Parvis

Dipartimento di Elettronica e Telecomunicazioni, Politecnico di Torino, Torino, ITALY

Luca Lombardo

Dipartimento di Elettronica e Telecomunicazioni, Politecnico di Torino, Torino, ITALY

DOI: 10.1109/MeMeA52024.2021.9478669

# Hydrogen chemoresistive sensor for the analysis of gut health

Alessio Gullino  
Sabrina Grassini  
*Dept. of Applied Science and Technology*  
*Politecnico di Torino*  
Torino, ITALY  
Email: alessio.gullino@polito.it

Kaveh Moulaei  
Nicola Donato  
*Dept. of Engineering*  
*University of Messina*  
Messina, ITALY  
Email: ndonato@unime.it

Giovanni Gugliandolo  
*Dept. MIFT*  
*University of Messina*  
Messina, ITALY  
Email: giovanni.gugliandolo@unime.it

Marco Parvis  
Luca Lombardo  
*Dept. of Electronics and Telecommunications*  
*Politecnico di Torino*  
Torino, ITALY  
Email: marco.parvis@polito.it

**Abstract**—Hydrogen is a target gas in the assessment of gut health. Several are the approaches to estimate the concentration of this gas, endogenously present in the gut and, of course, in the blood and the exhaled breath. In this paper, development and characterization of a resistive gas sensor for hydrogen monitoring is reported. The sensing material is based on Nb<sub>2</sub>O<sub>5</sub>–Pt thin films, obtained by depositing a niobium oxide layer and a platinum one on a tiny alumina substrate, by means of a lab-scale plasma sputtering reactor. The deposited layers were treated with a thermal process at 600 °C for 30 min. The developed devices were characterized in a hydrogen concentration range of 2000 ppm to 80000 ppm, showing promising results.

**Index Terms**—Hydrogen monitoring, gas sensors, chemoresistive sensors, thin films, gut, non-invasive techniques.

## I. INTRODUCTION

The chemical components of gut constitute the perfect fingerprint for the health of the human body. In particular, the gas inside the intestinal tract is an excellent indicator of the microbiota that naturally inhabit our gut. Small changes in the bacterial population can have a strong influence on the health. On the other hand, the alteration in the intestine flora can be a consequence of a severe illness like colon-rectal cancer [1]. For this reason, the analysis of the gas components produced in gut provides a clear picture of the bacterial activity and can be used in the diagnostics of gut disorders. Moreover, such analysis can provide new insight for the therapeutic treatment of several human diseases [2].

Although the gas in the stomach has a similar composition of the atmospheric air (i.e., 78% N<sub>2</sub> and 21% O<sub>2</sub>), inside the gut the gas composition is extremely variable [3]. However, the main components are oxygen O<sub>2</sub>, nitrogen N<sub>2</sub>, carbon dioxide (CO<sub>2</sub>), hydrogen (H<sub>2</sub>) and methane (CH<sub>4</sub>). They come from swallowed air and from the interaction of intestinal bacteria with undigested food. Altered levels of such gases can be

associated to health alterations. As an example, an abnormal production of hydrogen inside the gut has been related to severe diseases. In particular, a decreased production of this gas by intestinal microbiota may be related with the development and progression of the Parkinson's disease [4]. On the contrary, the production of hydrogen increases significantly in patients with ankylosing spondylitis, suggesting that gas in excess could be related to the intestine inflammation [5].

Analyzing the chemical makeup of gas produced by gut bacteria is not an easy task. Often, breath analysis is preferred since it is not invasive and provides a useful indicator of the intestinal gas. In fact, gases produced by the gut are partly adsorbed by the gut mucosa. Such gases, reaching the lung through the blood stream, are subsequently expelled with the exhaled breath. This technique is simple and non-invasive, however, it does not provide the origin of the gas species and, typically, measurements are not enough accurate [2], [6].

Whole body calorimetry, tube insertion and flatus analysis [7]–[9] are typical techniques used for gut gas analysis, however, they are often invasive [2]. The gas measurement from in-vitro incubation of fecal samples has been proposed as a non-invasive method. The samples are collected and placed in sealed containers with gas sensors in order to evaluate the gas species produced from fermentation [6]. The main advantage of this technique is that the samples can be collected easily and the bacterial population in feces is the same present in the intestine tract [6].

A relatively new approach consists in the ingestion of an electronic capsule equipped with a sensor able to track the gas content in the human intestine [2]. This technique allows one to take measurements of gas species from the stomach to the rectum and it has been successfully tested in some volunteers.

By considering the hydrogen monitoring techniques for gut

TABLE I  
MAIN INVESTIGATION TECHNIQUES FOR GUT H<sub>2</sub> DETECTION.

Technique	Ref	Maximum H <sub>2</sub> concentration (ppm)
Electronic capsule	[2]	40000
Hydrogen breath test	[10]	40
Tube insertion	[8]	50000
Samples fermentation	[11]	22500

health assessment, we can identify four concentration ranges, reported in Tab. I, and three main investigation techniques: breath analysis, in-situ monitoring, and gas monitoring during in-vitro incubation of fecal samples.

In such a context, the choice of the sensing device it is of primary importance. Of course, the right device must fulfill requirements such as: high sensitivity, excellent selectivity, and fast response/recovery times. Moreover, if the sensor must be employed for in-situ monitoring, it must satisfy low power consumption constraints, in order to be biased with small batteries, and it should feature small dimensions. Furthermore, all these requirements, closely depend on the employed sensing material, and its preparation should be compatible with microelectronic technologies, in order to scale dimensions of the device toward MEMs realization.

## II. CONDUCTOMETRIC GAS SENSORS

Among several gas sensors, conductometric gas sensors are gaining importance in different fields including biomedical applications [12]–[14]. Actually, they are characterized by low production costs, small dimension, and quite low power consumption combined with the possibility to customize and tailor the sensing properties of the sensor toward a specific target gas [16]. All these properties make conductometric gas sensors a suitable option to implement smart measurement systems for gut health assessment. In particular, they are suitable for the development of portable sensing devices due to their small dimension and low power consumption [17].

Conductometric gas sensors are formed by two inter-digitate electrodes connecting a sensing film, generally a metal oxide (MOX) film, which is deposited on them. The sensing mechanism is based on the presence of surface vacancies and broken bonds, which are able to adsorb gas molecules from the environment, acting as chemi-adsorption sites. In open air, oxygen species are generally adsorbed by such sites, causing the generation of a depletion layer that decreases the sensing film conductivity by trapping electrons from the conduction band. In the presence of a target gas, the adsorbed oxygen species are removed from the surface sites and replaced with the target molecules. Trapped electrons are released again into the conduction band causing a change in the film conductivity. In this way, it is possible to assess the resistance variation by employing a dedicated read-out system and extracting the sensor response by:

$$S = \frac{R_a}{R_g} \quad (1)$$

where  $R_a$  is the baseline resistance measured at open air condition and  $R_g$  is the resistance measured in presence of the target gas.

Nevertheless, metal oxide sensing layers are typically characterized by high electrical resistance (of the order of several gigaohms) at room temperature. This makes difficult to obtain high accuracy measurements due to the limitations of the readout system and the effects of noise. To avoid this problem, it is necessary to work at high temperature, generally in the range of 100 °C to 600 °C, in order to decrease the metal oxide resistance. Furthermore, temperature plays an important role on the control of the chemi-adsorption mechanisms. It is, therefore, important to detect a suitable working temperature in order to obtain the best tradeoff between sensing performance and power consumption.

The sensing film can also be enriched with noble particles in order to improve the sensitivity and selectivity toward a specific target gas. In particular, Pt can be used for increasing sensitivity and selectivity of H<sub>2</sub> gas detection [18], [19].

In this work, two conductometric gas sensors, based on a layer of niobium pentoxide (Nb<sub>2</sub>O<sub>5</sub>) enriched with platinum (Pt) nanoparticles, are characterized in terms of sensing performance toward hydrogen.

## III. SENSOR REALIZATION

The proposed sensors are manufactured on a small alumina substrate whose dimensions are about 6 mm × 3 mm. As shown in Fig. 1-A, a couple of platinum interdigitated electrodes are realized on the top side by screen printing deposition. In order to control the sensor working temperature, a Pt heater is present on the back side. The heater has been calibrated following the procedure discussed in [20], since the screen printed heater strips are characterized by a porous

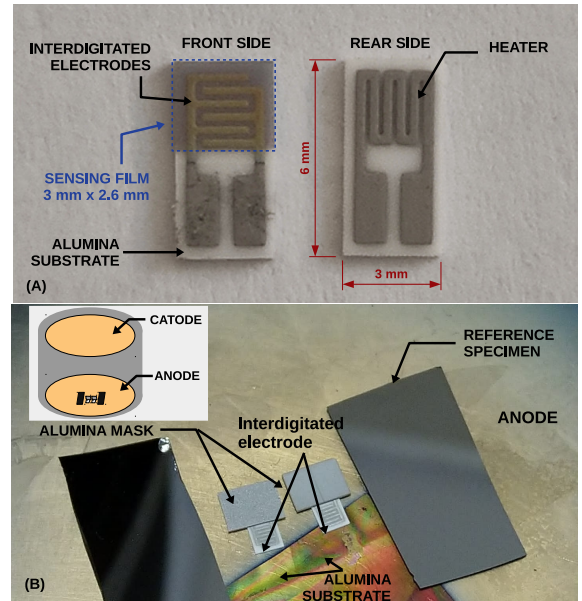


Fig. 1. (A) Front and rear sides for one of the realized sensors; (B) deposition setup of the alumina substrates inside the plasma sputtering reactor.

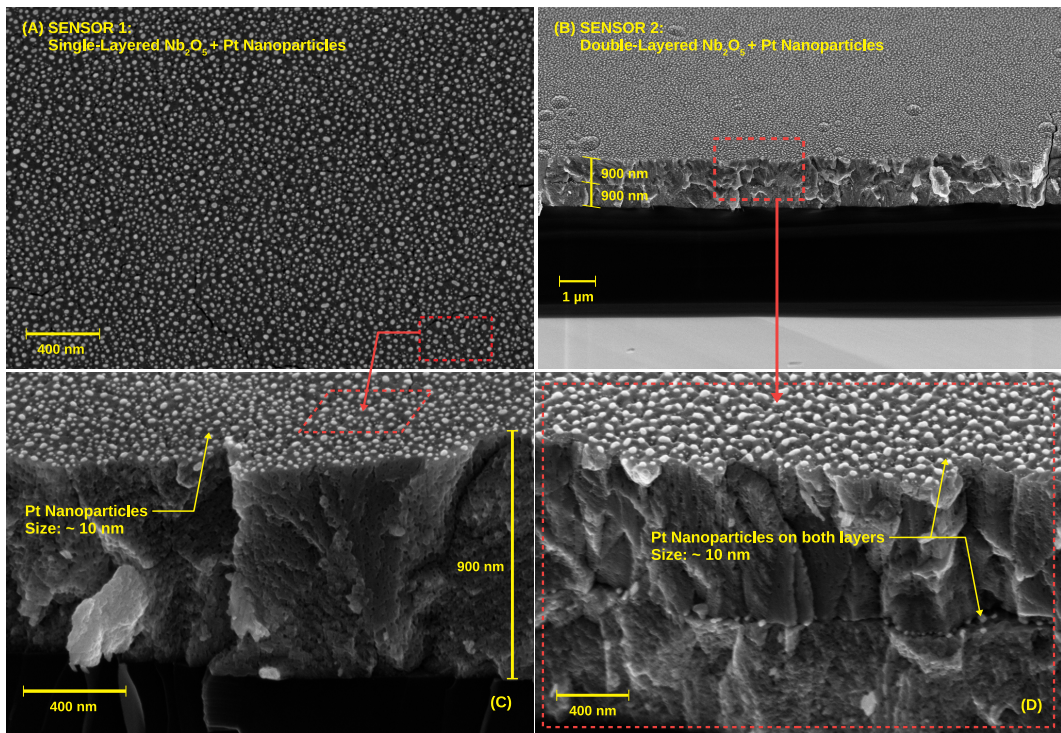


Fig. 2. Morphology of the deposited films for both the single-layer structure of sensor #1 (A,C) and the double-layer structure of sensor #2 (B,D).

structure which does not allow one to use a simple Calendar Van-Dusen equation for the estimation of their resistivity-temperature relation.

The sensing films are obtained by means of two different sputtering depositions which are carried out on the interdigitate electrodes. The first deposition is devoted to obtain the  $\text{Nb}_2\text{O}_5$  sensing film while the second one concerns the deposition of a platinum thin layer.

The  $\text{Nb}_2\text{O}_5$  thin film is obtained by a reactive plasma sputtering deposition employing a capacitively-coupled parallel-plate reactor with a RF frequency of 13.56 MHz. The circular deposition chamber is equipped with an anode electrode on the bottom and a cathode electrode located on the top, on which a pure Nb target (99.99% purity) is fixed. As shown in Fig. 1-B, the alumina substrates are located in the middle of the anode with the top side pointing toward the target and with a proper alumina mask placed over the contacts in order to protect them from the deposition and to obtain a well-defined sensing area of about  $3 \text{ mm} \times 2.6 \text{ mm}$ . The alumina substrates feature a rough surface which is not suitable for assessing the morphology of the deposited films. For this reason, two silicon wafer reference specimens, featuring a suitable smooth surface, are placed inside the deposition chamber beside the substrates. The deposition is performed in oxidative atmosphere composed of argon and oxygen (70% Ar, 30%  $\text{O}_2$ ) and employing a RF-power of 500 W for a total deposition time of 60 min.

Subsequently, a very thin layer of Pt is deposited over the  $\text{Nb}_2\text{O}_5$  sensing film by DC sputtering (QUORUM; model:

Q150T S) in an Ar inert atmosphere by employing a deposition power of  $30 \mu\text{A}$  for 10 s.

Both sensors are realized by using the same deposition parameters. Nevertheless, sensor #1 is characterized by a single  $\text{Nb}_2\text{O}_5$  film enriched with Pt nanoparticles, while the sensor #2 is characterized by a sandwich structure obtained repeating twice both the depositions of  $\text{Nb}_2\text{O}_5$  and Pt layers.

A final heat treatment was carried out by means of a tubular furnace (Thermo-Scientific; model: Lindberg/blue M) in an Ar inert atmosphere at  $600 \text{ }^\circ\text{C}$  for 30 min. Such a thermal treatment rearranged the Pt layer morphology creating very small nano-agglomerates on the  $\text{Nb}_2\text{O}_5$  film surface.

#### IV. MORPHOLOGICAL CHARACTERIZATION

Morphology and thickness characterization has been carried out by means of a Field Emission Scanning Electron Microscopy (FESEM - Supra 40 Zeiss) on the silicon wafer reference specimens deposited together with the sensors. Fig. 2 shows structure and the surface morphology for both sensors #1 and #2. In particular, the characterization reveals a quite similar morphology for all the  $\text{Nb}_2\text{O}_5$  thin films, which feature a porous structure and a thickness of about 900 nm.

On the surfaces it is possible to observe a homogeneous distribution of the Pt nanoparticles obtained after the thermal treatment. Such nanoparticles show a circular shape with an average diameter of about 10 nm. Sensor #2 is characterized by a  $\text{Nb}_2\text{O}_5$  double layer, separated by the Pt nanoparticles, which also in this case have an average diameter of about 10 nm. The overall film thickness is determined only by the  $\text{Nb}_2\text{O}_5$  layers, making the contribution of the platinum layer

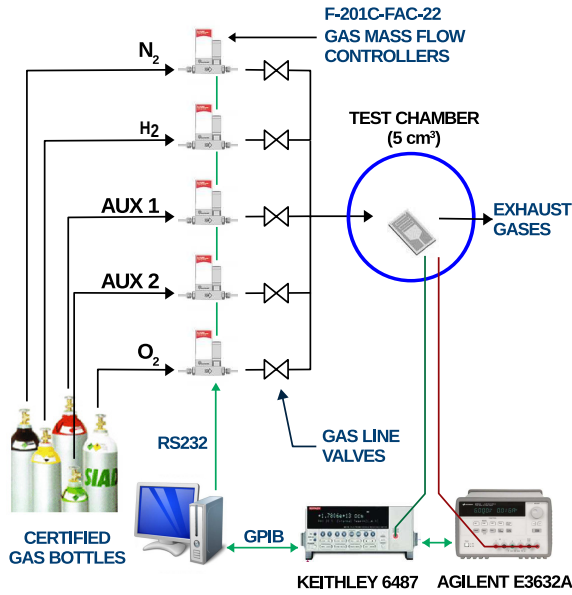


Fig. 3. Block diagram of the test-bench employed for the characterization of the proposed sensors.

negligible. Actually, film thicknesses are about 900 nm and 1800 nm for sensor #1 and #2, respectively.

## V. SENSING PERFORMANCE

The sensing performance characterization for the proposed sensors was carried out by means of an automated test-bench, specifically designed for the characterization of conductometric gas sensors. The block diagram of the test-bench is shown in Fig. 3. The setup is composed by a series of mass flow meters (BRONKHORST, model: F-201C-FAC-22) connected to certified gas cylinders. The mass flow meters, featuring an uncertainty of 2%, are controlled by a dedicated software in order to obtain a suitable gas mixture which flows inside a test chamber of about 5 cm<sup>3</sup>, suitable to obtain a fast response toward the variation of the target gas. The sensors working temperature is controlled by a bench power supply (AGILENT, model E3632A) connected to the Pt sensor heater, which acts both as heating element and as temperature probe. A picoammeter/voltage source (AGILENT, model 6487) is employed for the sensor resistance measurement.

### A. Optimal working temperature

First characterization is devoted to assess the working temperature at which the sensors exhibit the best sensing performance towards H<sub>2</sub>. With this aim, each sensor was tested at different temperatures, in the range of 150 °C to 400 °C in six steps. Synthetic air composed by 80% of N<sub>2</sub> and 20% of O<sub>2</sub> was employed as carrier gas. At each temperature step, 2000 ppm of H<sub>2</sub> were injected in the test chamber by means of a dedicated valve. Experimental data obtained for both sensors are shown in Fig. 4.

Both sensors exhibit a similar trend since the responses are lower at high temperature (400 °C) and gradually they increase reducing the working temperature until 150 °C, where

highest responses were detected. Even though best sensitivities appear at lower temperatures, two important considerations have to be taken into account:

- 1) Baseline resistance at 150 °C is about 52 GΩ and 9.3 GΩ for sample #1 and #2, respectively. Such resistance are quite high to be measured by low-cost portable devices.
- 2) At such a high resistance, noise starts to affect the signal acquisition with a significant degradation of the measurement accuracy.

For these reasons, a temperature of 200 °C has been chosen as optimal working temperature for both the proposed sensors. At this temperature sensors exhibit very good sensitivities and low power consumption. The baseline resistance is about 5 GΩ and 1.7 GΩ for sensor #1 and #2, respectively.

Responses as a function of working temperature, extrapolated by using Eq. 1, are shown in Fig. 4 (right graph). It is clear that sensor #1, characterized by a single layer, achieves the best results in terms of sensing response over the entire temperature range.

### B. Sensitivity toward hydrogen

After detecting the optimal working temperature, the sensors sensitivity toward hydrogen has been assessed. For this characterization, a constant synthetic air flux (80% N<sub>2</sub> and 20% O<sub>2</sub>) was used as carrier for flowing hydrogen pulses, with concentrations in the range of 2000 ppm to 80000 ppm. Sensors were exposed to the different concentrations at a working temperature of 200 °C, and the relative responses were collected. Experimental data, for both sensors, are shown in Fig. 5 (first and second plots).

From such data, the responses of both sensors as function of hydrogen concentration were computed by employing Eq. 1. As result, the calibration curves of the proposed sensors are shown in Fig. 5 (right plot). It is clear that both sensors achieve interesting sensitivities over a wide range of hydrogen concentration.

Moreover, an almost linear response can be observed for both sensors in the range of 2000 ppm to 10000 ppm, with sensor #1 reaching a response between 890 and 7700. This is an important feature of the proposed sensors, since the typical hydrogen concentration correlated to gut diseases lies in such a range. This simplifies both the sensor calibration and its employment in applications related to gut diseases.

At higher concentrations, the responses continue to increase with a second order behavior, meaning that the sensors start to be saturated by the target gas. This behavior is observed especially for sensor #2, whose calibration curve exhibits a marked bend for concentration higher than 10000 ppm.

In conclusion, both sensors exhibit excellent sensing responses toward hydrogen. In particular sensor #1 exhibits a higher response over the entire concentration range. Furthermore, the linear responses in the range of 2000 ppm to 10000 ppm makes such sensors very suitable for monitoring the intestinal hydrogen in diagnostic applications.

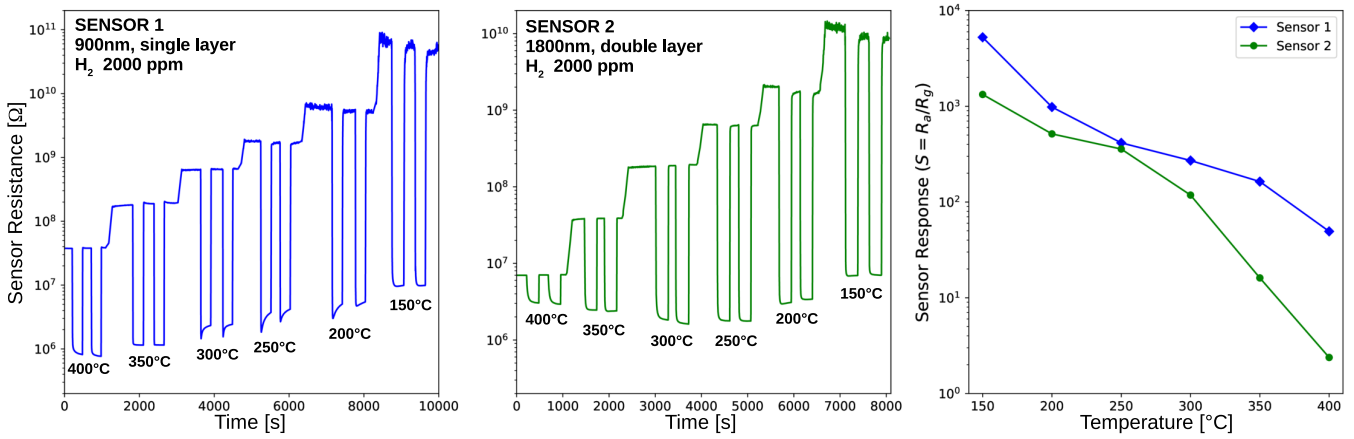


Fig. 4. Sensitivity characterization at different working temperatures in the range of 150 °C to 400 °C for sensor #1 and sensor #2.

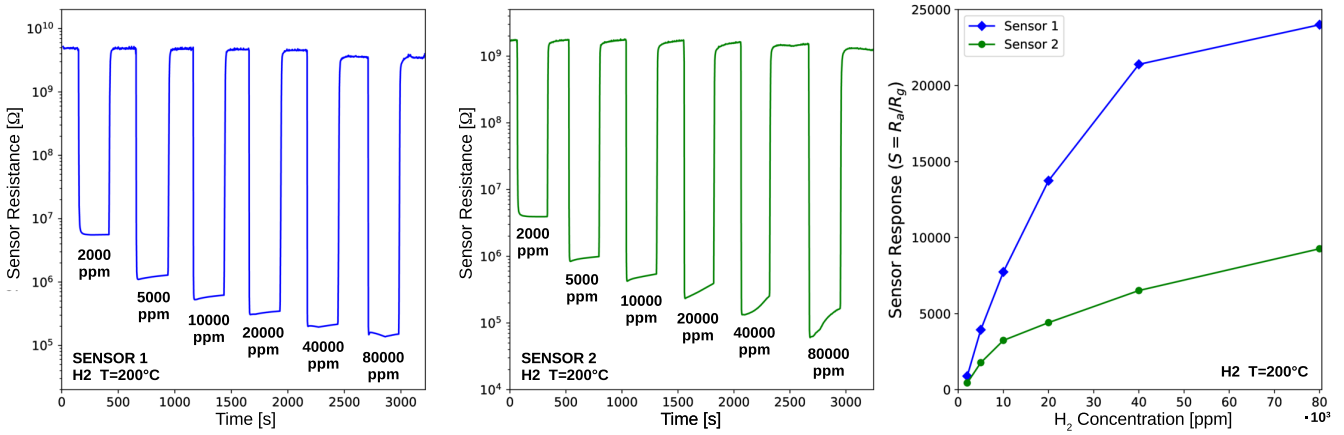


Fig. 5. Responses of sensor #1 and #2 toward different concentration of H<sub>2</sub> in the range of 2000 ppm to 80000 ppm at a working temperature of 200 °C.

### C. Sensor stability

It is extremely important that a sensor is able to guarantee response repeatability over time also after a continuous and repeated use. In fact, possible sensing film surface modifications, due to a prolonged use, can affect the response mechanism toward the target gas. The main consequence of such modifications is a degradation of the sensor stability and an increasing of its uncertainty. A good stability, therefore, avoids the necessity of frequently carrying out expensive calibrations of the sensor.

With the aim of assessing the repeatability of the proposed sensors, a further test was performed limiting the measurements only to sensor #1, since it achieved the best sensing performance towards hydrogen.

The sensor was placed inside the chamber under a constant flow of synthetic air flux (80% N<sub>2</sub> and 20% O<sub>2</sub>) and periodically exposed to hydrogen pulses at concentration of 2000 ppm. The working temperature was set at 200 °C and the data were acquired over a long period. As an example, Fig. 6 shows four repeated peaks where it is possible to observe a good repeatability of the sensor with almost no offset

TABLE II  
RESULTS OF THE STABILITY TEST CARRIED OUT WITH THE SENSOR #1.

Sensor Parameter	Average Value ( $\mu$ )	Relative Error ( $\epsilon$ )
Response ( $R$ )	910	1%
Baseline Resistance ( $R_a$ )	5.02 G $\Omega$	2%
Resistance ( $R_g$ )	5.55 M $\Omega$	1%

and hysteresis in the response.

From the stability test the average values and the relative errors, obtained as ratio between the absolute error and the expected value, were extrapolated for the response,  $R_a$  and  $R_g$ . The results are summarized in Table II and exhibit an average response of about 910 toward a concentration of 2000 ppm of H<sub>2</sub> with a relative error of 1%. Regarding the  $R_a$  and  $R_g$ , average values respectively of 5.02 M $\Omega$  and 5.55 M $\Omega$ , and with relative errors of 2% and 1%, respectively are obtained, confirming the good stability of the proposed sensor.

## VI. CONCLUSIONS

This work presents development and characterization of

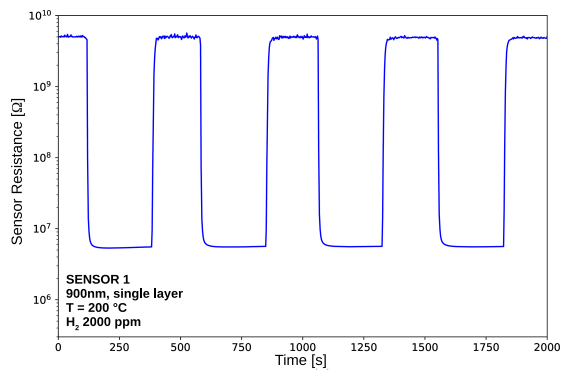


Fig. 6. Response of sensor #1 toward repeated  $H_2$  pulses at a concentration of 2000 ppm.

a resistive gas sensor for hydrogen monitoring. The sensor prototypes are based on  $Nb_2O_5$  thin films and Pt nanoparticles deposited via plasma sputtering on tiny alumina substrates. The first deposition is devoted to obtain the main film of  $Nb_2O_5$ , with a thickness of about 900 nm. Then, a very thin layer of platinum (few nanometers) is deposited on the first film and subsequently thermally cured in order to create the Pt nanoparticles layer. The two proposed sensors have different structures: sensor #1 is composed by a single-layer of  $Nb_2O_5$ -Pt nanoparticles, while sensor #2 have a double-layer structure of  $Nb_2O_5$ -Pt nanoparticles.

The sensing performances were assessed at different temperatures and in the presence of different hydrogen gas concentrations. It was observed that the best working temperature was 200 °C for both the sensors, since it allows to obtain a good compromise between sensitivity and power consumption.

The sensing characterizations show interesting results in terms of sensor response toward  $H_2$ . Actually, both sensors exhibit noteworthy responses in a range of concentration from 2000 ppm to 40000 ppm. Such results are promising, especially compared with the responses achieved by other different sensors present in literature [21].

Furthermore, the sensors exhibit excellent sensitivity toward hydrogen with an almost linear response up to 10000 ppm. In particular, sensor #1 exhibits the best results and, therefore, the double-layer structure does not lead to any advantage in such kind of sensor. Eventually, the stability of sensor #1 was assessed and the results demonstrate a good repeatability of the response over time with a relative error of about 1%.

In conclusion, the characterization of sensor #1 reveals the best properties for hydrogen detection making it a suitable candidate for the implementation of portable devices for monitoring gut diseases due to its excellent sensing performance, small size and low power consumption. It is also confirmed by the comparison of the achieved results with respect to the performance of a commercial hydrogen sensor (MIXEN, model: MIX8417), which is able to detect a maximum  $H_2$  concentration of 2000 ppm with an uncalibrated sensitivity uncertainty of about 50% [22].

## REFERENCES

- [1] A. Ishibe, M. Ota, A. Takeshita et al., Detection of gas components as a novel diagnostic method for colorectal cancer, *Ann Gastroenterol Surg.*, 2018, Vol. 2, pp. 147–153, <https://doi.org/10.1002/ags3.12056>.
- [2] K. Kalantar-Zadeh, K. J. Berean, N. Ha et al., A human pilot trial of ingestible electronic capsules capable of sensing different gases in the gut, *Nat. Electron.*, 2018, Is. 1, pp. 79–87, <https://doi.org/10.1038/s41928-017-0004-x>.
- [3] M. D. Levitt and J. H. Bond Jr., Volume, composition, and source of intestinal gas, *Gastroenterology*, 1970, Vol. 59:6, pp. 921–929.
- [4] A. Suzuki, M. Ito, T. Hamaguchi, H. Mori, Y. Takeda, R. Baba et al., Quantification of hydrogen production by intestinal bacteria that are specifically dysregulated in Parkinson's disease, *PLoS ONE*, 2018, 13(12), <https://doi.org/10.1371/journal.pone.0208313>.
- [5] L. Shang, T. Zhang, X. Liu et al., AB0034 increased production of hydrogen and methane suggested bacterial overgrowth in the small intestine in patients with autoimmune disease detected by lactulose breath test, *Annals of the Rheumatic Diseases*, 2019, Is. 78, pp. 1482–1483.
- [6] A. Rotbart et al., Designing an in-vitro gas profiling system for human faecal samples, *Sensors and Actuators B: Chemical*, 2017, Is. 238, pp. 754–764.
- [7] D. Merriman, R. Wright, P. J. Traynor, Whole body indirect calorimetry (human calorimetry) gas analysis by mass spectrometry, 2008.
- [8] M. D. Levitt, Volume and composition of human intestinal gas determined by means of an intestinal washout technic, *New England Journal of Medicine*, 1971, Is. 284:25, pp. 1394–1398.
- [9] J. Tomlin, C. Lowis, N. W. Read, Investigation of normal flatus production in healthy volunteers, *Gut*, 1991, Is. 32:6, pp. 665–669.
- [10] U. C. Ghoshal, How to interpret hydrogen breath tests, *Journal of neurogastroenterology and motility*, The Korean Society of Neurogastroenterology and Motility, 2011, Vol. 17, No. 3, doi: 10.5056/jnm.2011.17.3.312.
- [11] K. Y. Chu, A. Rotbart, Z. O. Jian, K. Kalantar-Zadeh et al., Modulation of colonic hydrogen sulfide production by diet and mesalazine utilizing a novel gas-profiling technology, *Gut Microbes*, 2018, Is. 9:6, pp. 510–522, doi: 10.1080/19490976.2018.1451280.
- [12] L. Lombardo et al.,  $Nb_2O_5$  thin film-based conductometric sensor for acetone monitoring, 2019 IEEE International Symposium on Medical Measurements and Applications, Istanbul, Turkey, 2019, pp. 1–5, doi: 10.1109/MeMeA.2019.8802126.
- [13] C. Wang, L. Yin, L. Zhang, D. Xiang, and R. Gao, Metal Oxide Gas Sensors: Sensitivity and Influencing Factors, *Sensors*, vol. 10, pp. 20882106, 2010.
- [14] Neri, G., Bonavita, A., Micali, G., Donato, N. (2009). Design and development of a breath acetone MOS sensor for ketogenic diets control. *IEEE Sensors Journal*, 10(1), 131-136.
- [15] J. Chen, J. Zhang, M. Wang, and Y. Li, High-temperature hydrogen sensor based on platinum nanoparticle-decorated SiC nanowire device, *Sensors Actuators B Chem.*, vol. 201, pp. 402406, 2014.
- [16] G. Korotcenkov and B. K. Cho, "Metal oxide composites in conductometric gas sensors: Achievements and challenges", *Sensors Actuators B. Chem.*, vol. 244, pp. 182210, 2017.
- [17] L. Lombardo, S. Grassini, M. Parvis, N. Donato, and A. Gullino, Ethanol breath measuring system, in *IEEE International Symposium on Medical Measurements and Applications - Bari 2020*.
- [18] Q. A. Drmash, Z. H. Yamani, A. K. Mohamedkhair, A. H. Y. Hendi, and A. Ibrahim, Room-temperature detection of hydrogen by platinum-decorated tin oxide thin films augmented by heat-treatment, *Vacuum*, vol. 156, pp. 6877, 2018.
- [19] J. Chen, J. Zhang, M. Wang, and Y. Li, High-temperature hydrogen sensor based on platinum nanoparticle-decorated SiC nanowire device, *Sensors Actuators B Chem.*, vol. 201, pp. 402406, 2014.
- [20] L. Lombardo et al., High Sensitive and Selective Minisensor for Acetone Monitoring, *IEEE Transaction on Instrumentation and Measurement*, 2020, Vol. 69, No. 6, pp. 3308–3316, doi: 10.1109/TIM.2020.2967161.
- [21] S. R. Gottam, C. Tsai, L. Wang, C. Wang, C. Lin, S. Chu, Highly sensitive hydrogen gas sensor based on a  $MoS_2$ -Pt nanoparticle composite, *Applied Surface Science*, Vol. 506, 2020, ISSN 0169-4332, <https://doi.org/10.1016/j.apsusc.2019.144981>.
- [22] MixSensors: <https://www.mixsensors.com> last checked on 2021-03-31.